

Multi-material Direct Ink Writing and Embroidery for Stretchable Wearable Sensors

Lukas Cha^{1,2}, Ryman Hashem^{1,2}, Ria Prakash¹, Tanguy Declyt^{1,3}, Wenze Zhang¹, and Liang He^{1,2}

Abstract—The development of wearable sensing systems for sports performance tracking, rehabilitation, and injury prevention has driven a growing demand for smart garments that combine comfort, durability, and accurate motion detection. This paper presents a textile-compatible fabrication method that integrates multi-material direct ink writing with automated embroidery to create stretchable strain sensors directly embedded onto garments. The process combines sequential printing of silicone, conductive carbon grease, and silicone encapsulation layers with embroidery that simultaneously provides mechanical attachment and electrical interconnection. The resulting hybrid sensor exhibits a high stretchability of 120% and demonstrates stable electromechanical performance with a linearity of $R^2 = 0.99$, gauge factor of 31.4, and hysteresis of 22.9%. Repeated loading-unloading tests over 80 cycles confirm a baseline and peak drift (0.135% and 0.236% per cycle, respectively), validating the sensor's repeatability. As a proof of concept, the sensor was integrated into wearable elbow and knee sleeves for joint-angle monitoring, showing a strong correlation between normalised resistance change ($\Delta R/R$) and bending angle. This hybrid fabrication route bridges printed stretchable electronics with conventional textile manufacturing, offering a reproducible, aesthetically compatible, and scalable pathway toward intelligent garments for motion capture and soft robotic applications.

Index Terms—soft sensors, fabrication, textiles, wearables

I. INTRODUCTION

The integration of stretchable sensors into textiles is a rapidly advancing field with significant implications for wearable electronics, soft robotics, and human–machine interaction [1]. In addition, these technologies play a crucial role in sports rehabilitation and performance monitoring, where real-time detection of joint movement and muscle activity can aid injury prevention and optimise athletic training [2]. Unlike rigid electronic components, stretchable devices can conform to the body’s natural motion, enabling accurate monitoring of physiological signals and joint kinematics without restricting movement [3]. Achieving this level of mechanical compliance while maintaining reliable electrical performance remains a key challenge for the development of next-generation smart garments [4].

Direct ink writing (DIW) has emerged as a versatile additive manufacturing technique for fabricating soft and stretchable

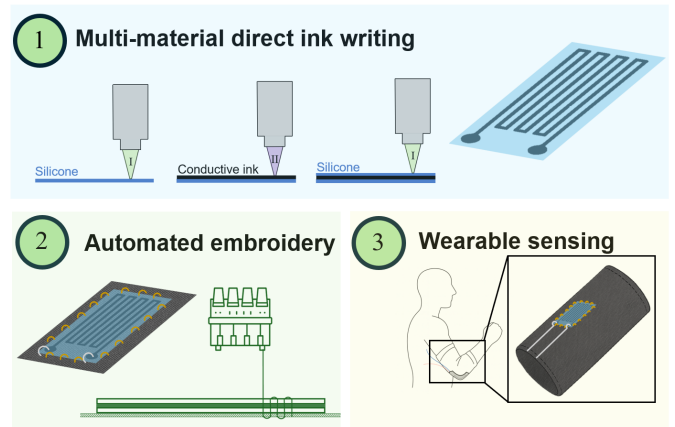


Fig. 1. (1) Multimaterial direct ink writing of silicone and conductive ink to form a soft, stretchable strain sensor. (2) Automated embroidery mechanically anchors the printed sensor to a textile substrate while simultaneously creating electrical interconnects. (3) The integrated system enables wearable motion sensing applications.

electronics [5]. It allows precise deposition of functional materials such as silicones, conductive composites, and hydrogels in custom geometries, offering excellent control over mechanical and electrical properties [5]–[7]. However, most DIW-based stretchable sensors are fabricated on planar substrates such as glass or polydimethylsiloxane (PDMS), which imposes a challenge with respect to their integration onto textiles. Conventional attachment techniques such as adhesives or heat lamination are often compromise the fabric’s breathability, comfort, and long-term durability [8].

To address these limitations, textile-based fabrication strategies such as weaving, knitting, and embroidery have gained attention for their ability to embed conductive pathways and sensors directly into fabrics [9]. Among these, embroidery provides high spatial precision, pattern flexibility, and compatibility with industrial-scale manufacturing [10]. Yet, combining embroidery with soft-material printing techniques for hybrid sensor fabrication remains relatively unexplored.

In this work, we present an embroidery machine-based approach that integrates stretchable strain sensors directly onto textiles, shown in Fig. 1. Regular thread provides mechanical fixation to the garment, while conductive thread interfaces with the printed conductive layer to enable robust electrical connection. This dual-function embroidery process achieves both mechanical and electrical integration within a single automated step, offering a scalable and repeatable route toward

*This work was supported by The Podium Institute for Sports Medicine and Technology, University of Oxford.

¹Institute of Biomedical Engineering, University of Oxford, United Kingdom

²The Podium Institute for Sports Medicine and Technology, University of Oxford, United Kingdom

³École Polytechnique Fédérale de Lausanne, Switzerland

All inquiries can be addressed to: lukas.cha@eng.ox.ac.uk

textile-embedded soft sensors.

We demonstrate the functionality of this system through mechanical stretchability and cyclic durability tests of the resulting sensor, as well as an application experiment measuring elbow and knee joint angles. The results show that the printed-embroidered sensor maintains stable performance under repeated strain and provides good motion detection. This method holds strong potential for smart textiles in sportswear, enabling the development of garments that enhance athletic performance through real-time motion tracking, physiological monitoring [2], while remaining both aesthetically compatible and functionally intelligent [11].

II. BACKGROUND

Wearable and garment-integrated strain sensors have attracted growing attention for applications in motion capture, health monitoring, and human-machine interaction. Existing textile-based sensors utilise a range of architectures—such as printed conductive films, conductive yarns, and hybrid composites—yet achieving seamless integration into garments that maintain both mechanical flexibility and stable electrical connectivity remains a significant challenge [12]–[14]. Below, current techniques to fabricate textile-based wearable sensors are outlined.

Printed resistive sensors on textiles. Screen and inkjet printing have produced high-performance strain sensors using carbon-, PEDOT:PSS-, or AgNW-based inks directly on fabric [12], [13]. These systems deliver wide working ranges (up to 200%) and long lifetimes (5000 cycles), with demonstrations on gloves and stretchable garments. Graphene-dyed textiles also exhibit distinctive negative resistance variations when deformed [15]. Despite industrial maturity and good electrical performance, these methods typically deposit a single conductive layer on fabric and rely on external wiring, lacking the encapsulated elastomer-conductor-elastomer stack or integrated embroidered interconnects that would enable mechanical robustness and washability.

Silicone-textile composites and encapsulated sensors. Several studies have introduced cast or laminated elastomer layers to encapsulate conductive fabrics or inks, improving mechanical stability and stretchability on textile substrates [14]. A representative work demonstrated silicone-encapsulated conductive fabric for elbow and respiration sensing with gauge factors around -1.1 and low hysteresis (3.2%). Such composites highlight the benefit of soft encapsulation but generally rely on manual casting and discrete connectors, rather than an automated fabrication process.

Embroidery and stitched sensors. Embroidery has emerged as a precise and scalable textile manufacturing method for placing conductive yarns in programmable patterns. Conductive-thread embroidery has been used to realise resistive strain sensors with zigzag or pre-strained patterns for knee, gait, and elbow monitoring [16], [17]. These studies demonstrate that stitch geometry and substrate elasticity significantly affect sensitivity and strain range (up to

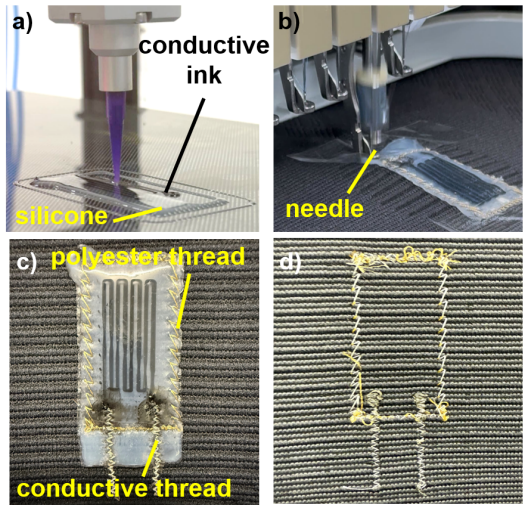


Fig. 2. Fabrication and integration of the printed strain sensor. (a) Direct ink writing process, in which the conductive ink is encapsulated between two silicone layers. (b) Automated embroidery step used to stitch and mechanically anchor the printed sensor to the fabric. (c) Front view of the integrated strain sensor showing the printed and stitched structure. (d) Back view illustrating the embroidered conductive interconnects.

60–70%). However, the embroidered thread typically functions as the sensor itself, not as an interface to a printed multilayer structure, leaving open the opportunity for hybrid printed-embroidered architectures.

Hybrid printed-embroidered interconnects. A smaller number of works explore the interface between printed conductors and embroidered threads, notably using overstitching of printed pads followed by overprinting or lamination to stabilise contact resistance under mechanical and thermal stress [18]. This approach directly addresses interconnect reliability, a common failure point in soft e-textiles, but has not yet been combined with printed elastomer-conductor stacks or demonstrated on garments with integrated motion sensing.

On-body validation and performance gaps. Across the literature, printed and embroidered sensors have been validated on-body for gestures and joint-angle tracking [12], [14], [16], [19]. Working strains span from 0–200%, and gauge factors vary widely depending on the conductive mechanism, with both positive and negative responses reported. Yet, explicit electrical failure criteria, cyclic drift data, and long-term embroidered-to-printed interconnect characterisation are rarely provided. Consequently, while the field demonstrates strong component technologies, a unified, garment-compatible process that co-registers printed and embroidered elements with full on-body evaluation remains unrealised. This gap motivates the present work, which combines direct ink writing of silicone–carbon grease layers with automated embroidery for simultaneous mechanical and electrical integration on fabric.

III. METHOD & FABRICATION

The fabrication framework, depicted in Fig. 1, is composed of a sensor printing stage and a fabric-attachment via em-

broidery stage. These two stages are shown in Fig. 2a and 2b, respectively.

Direct Ink Writing (DIW) of Multilayer Stretchable Sensor. The stretchable strain sensor was fabricated using a modified Ender 5 Plus 3D printer equipped with two *Vipro 3* (Viscotec, Germany) progressive cavity pump printheads, controlled using a Duet 3 mini+ (Duet3D, United Kingdom) board. The printheads are both equipped with a 0.51 mm nozzle, resulting in the same printed line width. Each printhead was dedicated to one material: conductive carbon grease (846-1P, MG Chemicals, Canada) and silicone (Ecoflex 00-30, Smooth-On, USA). The printheads were mounted on a custom-designed rack with linear guides actuated pneumatically as shown in Fig. 3, enabling vertical motion to lift the inactive nozzle and lower the active nozzle during printing to prevent undesired surface contact. A custom-built syringe-pushing rig continuously mixed Ecoflex 00-30 Part A and Part B using a static mixer, feeding the blend to the silicone printhead via a flexible tube. Ecoflex 00-30 was selected for its high elongation and compliance in the cured state. The printing sequence comprised three layers: (1) a 0.3 mm silicone base layer printed at 10 mm/s onto the textile substrate, (2) a 0.3 mm patterned layer of conductive carbon grease deposited on the semi-cured silicone, and (3) a 0.3 mm silicone encapsulation layer extruded with an elevated nozzle clearance (additional 0.7 mm elevation) to avoid smearing the underlying conductor. The print bed was maintained at 60 °C to accelerate partial curing of the first layer and ensure structural integrity before deposition of subsequent layers. The complete three-layer sensor was printed within approximately 20 minutes. Fig. 2a depicts the printing. The size of the strain sensor is 25 mm × 58 mm with a strain gauge pattern of dimension 13 mm × 30 mm and line width 0.51 mm. This conductive trace geometry resulted in a baseline resistance of 2.5 MΩ. Due to the continuous premixing setup, the silicone feed required purging every two minutes to refresh material and maintain stable viscosity, as the mixed Ecoflex 00-30 gradually increased in viscosity within the tubing and printhead.

Embroidery-Based Integration onto Fabric. The printed sensor was integrated onto textile using a PR1055X embroidery machine (Brother, Japan), with stitching patterns designed in Hatch 3 embroidery software (Wilcom, USA). The CAD design of the garment section was imported into Hatch 3, allowing precise placement of embroidery regions relative to the printed sensor. A positional marker sticker was placed on the sensor edge, which was detected by the embroidery machine's onboard camera for automatic alignment within the embroidery hoop. Initially, the sensor was fixed in a pre-stretched state on the fabric using tape, and its perimeter was mechanically secured with standard thread stitches along all four sides. Along the top and bottom sides of the sensor, a dense stitch pattern was chosen for mechanical strength. For the left and right edges of the sensor, a zig-zag pattern of width 3 mm was chosen such that the stitch does not limit the stretchability of the elastic sportswear fabric. Following mechanical fixation, conductive thread was used to embroider

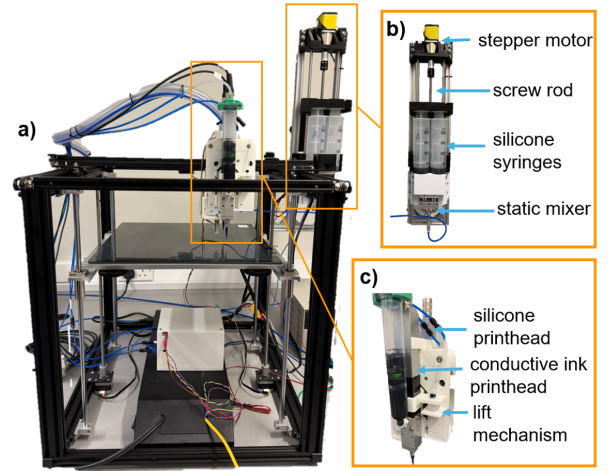


Fig. 3. Custom multimaterial 3D printing system. (a) Overview of the modified printer structure based on a Creality Ender 5 Plus platform. (b) Syringe-pushing assembly for silicone extrusion, where a stepper motor drives a screw rod to dispense and mix the two silicone components (Parts A and B) via a static mixer. (c) Dual printhead rack featuring separate printheads for silicone and conductive ink; a pneumatic lift mechanism selectively lowers the active printhead during printing.

electrical traces from the conductive pad region of the sensor to external contact points interfacing with a multimeter for signal acquisition. This embroidery process achieved both mechanical anchoring and electrical interfacing, ensuring a robust and repeatable integration of the stretchable printed sensor onto the garment substrate. The front and back sides of the resulting sensor are shown in Fig. 2c and Fig. 2d.

IV. EXPERIMENTAL SETUP AND DESIGN

Sensor Characterisation with Tensile Tester. The mechanical and electrical performance of the printed-embroidered strain sensor was characterised using a tensile tester (Mark-10, USA). The sensor was mounted on an 28 mm × 100 mm fabric sample and electrically connected to an LCR meter (GW-Instek 6020, Taiwan) that continuously recorded resistance changes at a sampling frequency of 10 Hz. In the first test shown in Fig. 4a, cyclic tensile loading was applied to the sample to measure electrical resistance as a function of strain and corresponding force. The test was conducted over 80 loading-unloading cycles at a displacement rate of 60 mm/min. This experiment evaluated the linearity, sensitivity, hysteresis, and drift of the fabric attached strain sensor under repeated mechanical deformation. In the second test, shown in Fig. 4b, a monotonic stretch to failure test was performed, where the sensor was elongated at a rate of 60 mm/min until mechanical or electrical failure occurred. This detachment/break test assessed the ultimate stretchability of the printed sensor and the robustness of the embroidered mechanical and electrical interconnections between the sensor and the textile substrate.

Elbow and Knee Angle Application Experiment. To demonstrate the sensor's capability for motion tracking, an application experiment shown in Fig. 4c was conducted using an embroidered sensor integrated onto an elastic elbow sleeve and

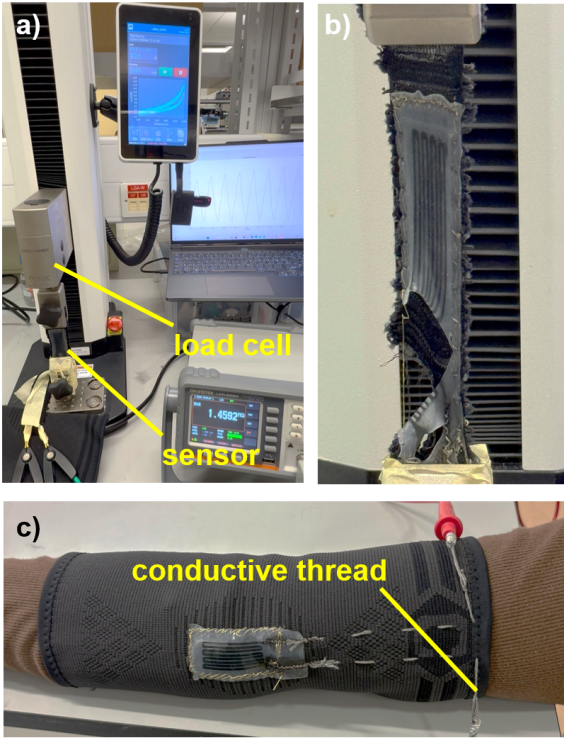


Fig. 4. Characterisation and demonstration of the printed strain sensor. (a) Tensile testing setup showing the sensor mounted on the universal testing machine. (b) Sensor condition after mechanical failure during the stretch-to-failure test. (c) Integration of the printed and embroidered sensor onto an elbow sleeve for wearable motion sensing.

elastic knee sleeve. The sensor was stitched in place using the embroidery machine and connected via conductive thread to an LCR meter (GW-Instek 6020, Taiwan) that recorded resistance at a frequency of 10 Hz. Measurements were taken at distinct, controlled elbow and knee angles to establish a calibration curve correlating normalised resistance change ($\Delta R/R$) with joint angle. A fully outstretched arm or leg was defined as 180 degrees. The calibrated relationship was then validated during dynamic motion. A video of the elbow movement was analysed using Python and the OpenCV computer vision framework to extract the actual elbow and knee angles frame by frame, which was compared against the sensor-estimated angles. This comparison allowed evaluation of the accuracy and temporal response of the embroidered, fabric integrated strain sensor in capturing human joint kinematics.

V. RESULTS AND DISCUSSION

This section presents the preliminary results of the cyclic strain and stretch-to-failure experiments, highlighting the sensor's linearity, sensitivity, hysteresis, stretchability and drift characteristics, summarised in Table I.

1) Hysteresis: To evaluate hysteresis behaviour, the stretch and release curves from the cyclic strain test were analysed. The relative resistance across strain is shown in Fig. 5. The resistive strain sensor exhibited a hysteresis of 22.9%, calculated from the ratio of the areas under the loading and unloading

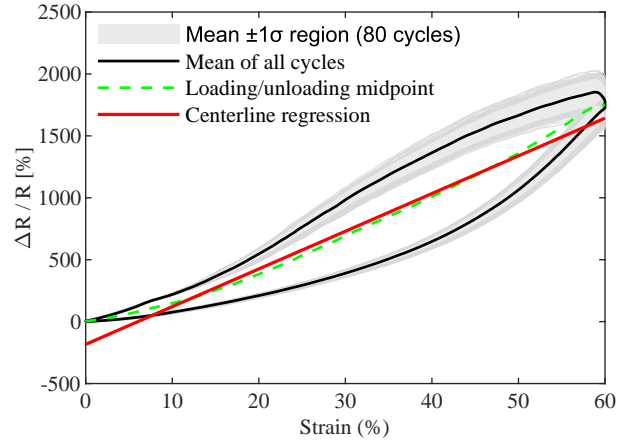


Fig. 5. Cyclic strain characterisation of the printed strain sensor. The black curve represents the mean of the load and unloading sections, while the grey shaded region indicates ± 1 standard deviation. The green dashed line shows the average midpoint between loading and unloading for each cycle, and the red line is the linear regression of this midpoint curve, used to evaluate sensor linearity and sensitivity.

curves [20]. This value is consistent with other resistive strain sensors utilising carbon-based conductive networks [20]. The observed hysteresis is attributed to viscoelastic effects within the elastomer matrix and the dynamic reformation and breakdown of conductive pathways in the carbon black percolation network [20], [21]. Future work will investigate alternative conductive inks and matrix formulations to reduce hysteresis and enhance repeatability.

TABLE I
SENSOR PERFORMANCE METRICS

Metric	Value
Linearity R^2	0.990
Sensitivity	31.42
Hysteresis [%]	22.90
Stretchability [%]	120
Rel. Baseline Drift/Cycle [%]	0.135
Rel. Peak Drift/Cycle [%]	0.236

2) Linearity and Sensitivity: Linearity and sensitivity were quantified from the midpoint curve averaged over all 80 cyclic loading-unloading cycles, as shown in Fig. 5. The coefficient of determination was found to be $R^2 = 0.99$, indicating highly linear behaviour. The sensitivity, defined as the slope of the linear fit, was $GF = 31.42$. These values demonstrate excellent linearity and gauge factor performance, comparable to the other silicone-carbon grease resistive strain sensors reported in the literature [22], [23].

3) Stretchability: The stretch-to-failure test results are shown in Fig. 6. The sensor exhibited stable and approximately linear behaviour up to 60% strain, beyond which the response became nonlinear, and the resistance decreased slightly. This behaviour is attributed to the mechanical rearrangement of the carbon black percolation network within the conductive grease [24]. Mechanical failure occurred at 120% strain, shown in Fig. 6. The corresponding force curve indicates that minimal

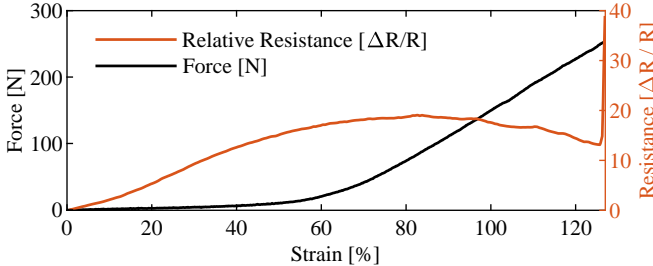


Fig. 6. Stretch-to-failure characterisation of the printed strain sensor. The blue curve (left y-axis) shows the applied force as a function of strain, while the orange curve (right y-axis) represents the corresponding change in relative resistance ($\Delta R/R$).

force (below 20 N) was required to stretch the sensor up to 60% strain, indicating that it would minimally affect wearer mobility when worn.

4) Cyclic Stability: The full 80-cycle test, shown in Fig. 7, demonstrates gradual drift of the sensor response over time. The relative baseline drift per cycle was 0.135%, while the relative peak drift per cycle was 0.236 % [25]. This behaviour highlights the influence of material relaxation and conductive ink composition on long-term stability. Future work will focus on comparing different conductive printable materials to minimise drift and improve durability during repeated deformation.

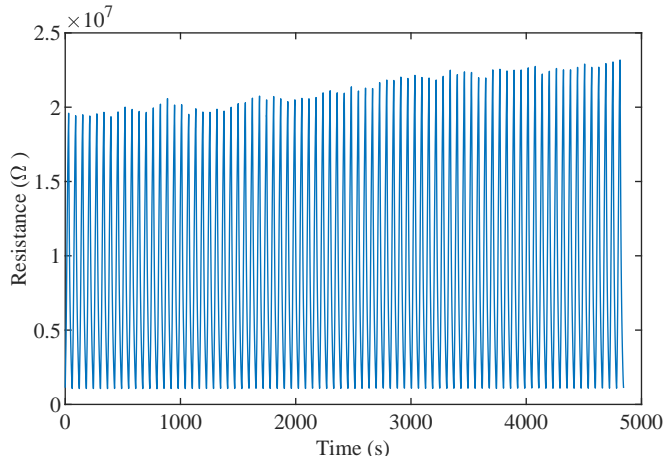


Fig. 7. Absolute resistance of the printed strain sensor over 80 cyclic loading-unloading cycles. The plot shows resistance (Ω) as a function of time, demonstrating consistent periodic response and stable electrical behaviour throughout repeated deformation.

5) Elbow and Knee Motion Experiment: Fig. 8a and Fig. 8b show the calibrated elbow and knee angle measurements obtained from the wearable strain sensors, benchmarked against ground-truth angle data derived from the OpenCV tracking algorithm. The mean absolute percentage error (MAPE) was 17.2% for the elbow and 17.9% for the knee. For the knee motion, a noticeable increase in error occurs at high flexion angles, where the sensor experiences larger strains. This behaviour is attributed to the sensor being stretched

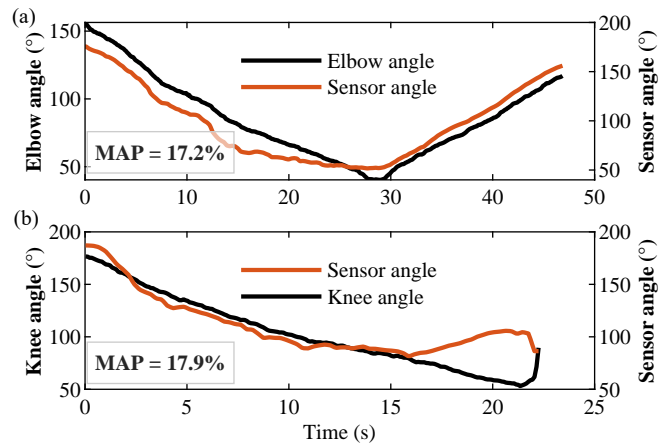


Fig. 8. Calibrated joint angle tracking. (a) Elbow and (b) knee angles measured by the sensor and the OpenCV ground-truth algorithm. The mean absolute percentage error (MAPE) is shown on each plot.

beyond its linear operating range of approximately 60% strain, where nonlinear sensor response leads to deviation from the true angle values. In contrast, the elbow motion induces a lower overall strain on the sensor, keeping it within its linear region and thus preventing similar deviation at higher bend angles. During the experiment, the sensor exhibited noticeable temperature sensitivity, requiring constant ambient conditions for stable operation. Future work will investigate alternative conductive materials to eliminate this dependence and enhance robustness. The mean absolute error of around 17 % is higher than state-of-the-art results for garment-integrated strain sensors, e.g. [3], [15], [17]. However, the present work primarily aims to demonstrate the fabrication framework rather than optimise sensing accuracy.

VI. CONCLUSION AND FUTURE WORK

This work demonstrates a hybrid fabrication strategy that integrates direct ink writing of silicone–carbon grease multi-layer sensors with automated embroidery for seamless textile integration. By combining multi-material additive manufacturing and embroidery-based attachment, both the mechanical and electrical interfaces are achieved within a single, automated workflow compatible with garment production. The resulting strain sensor exhibits a total stretchability of up to 120%, maintaining reliable conductivity throughout deformation. Preliminary sensor characterisation revealed a linear resistance–strain relationship with an R^2 of 0.99, and a hysteresis error of 22.9% and sensitivity of 31.41. When applied as an elbow-angle sensor, the device shows good tracked joint motion, showing clear correlation between sensor resistance and flexion angle, validating its potential for body-motion monitoring. The integration process enables robust, repeatable, and aesthetically compatible soft sensors on fabric. Overall, this approach bridges the gap between printed stretchable electronics and wearable textiles, offering a practical pathway toward next-generation smart garments for sports, rehabilitation, and interactive applications.

Future work aims to explore alternative conductive materials such as liquid metal to improve the sensor characteristics and explore capacitive strain sensing in this framework. Various stitch patterns will be studied and compared, testing their effect on overall sensor stretchability. Additionally, strain sensor array designs to capture multiple degrees-of-freedom of human joints will be investigated.

ACKNOWLEDGMENT

The authors would like to thank Massimo Mariello from the Oxford Bioelectronics Lab for his help with the tensile tester.

REFERENCES

- [1] J. Xiong, J. Chen, and P. S. Lee, “Functional fibers and fabrics for soft robotics, wearables, and human–robot interface,” *Advanced materials*, vol. 33, no. 19, p. 2 002 640, 2021.
- [2] R. De Fazio, V. M. Mastronardi, M. De Vittorio, and P. Visconti, “Wearable sensors and smart devices to monitor rehabilitation parameters and sports performance: An overview,” *Sensors*, vol. 23, no. 4, p. 1856, 2023.
- [3] O. Atalay, “Textile-based, interdigital, capacitive, soft-strain sensor for wearable applications,” *Materials*, vol. 11, no. 5, p. 768, 2018.
- [4] J. Wang, C. Lu, and K. Zhang, “Textile-based strain sensor for human motion detection,” *Energy & Environmental Materials*, vol. 3, no. 1, pp. 80–100, 2020.
- [5] N. C. Brown, D. C. Ames, and J. Mueller, “Multimaterial extrusion 3d printing printheads,” *Nature Reviews Materials*, pp. 1–19, 2025.
- [6] K. Yamagishi, R. Karyappa, T. Ching, and M. Hashimoto, “Direct ink writing of silicone elastomers to fabricate microfluidic devices and soft robots,” *MRS Communications*, vol. 14, no. 5, pp. 846–861, 2024.
- [7] M. Ho, A. B. Ramirez, N. Akbarnia, *et al.*, “Direct ink writing of conductive hydrogels,” *Advanced Functional Materials*, vol. 35, no. 22, p. 2 415 507, 2025.
- [8] L. Sanchez-Botero, A. Agrawala, and R. Kramer-Bottiglio, “Stretchable, breathable, and washable fabric sensor for human motion monitoring,” *Advanced Materials Technologies*, vol. 8, no. 17, p. 2 300 378, 2023.
- [9] J. Pu, K. Ma, Y. Luo, *et al.*, “Textile electronics for wearable applications,” *International Journal of Extreme Manufacturing*, vol. 5, no. 4, p. 042 007, 2023.
- [10] Y. Yang, Y. Chen, Y. Liu, and R. Yin, “Programmable and scalable embroidery textile resistive pressure sensors for integrated multifunctional smart wearable systems,” *Advanced Fiber Materials*, vol. 7, no. 2, pp. 574–586, 2025.
- [11] E. Ismar, S. Kurşun Bahadir, F. Kalaoglu, and V. Koncar, “Futuristic clothes: Electronic textiles and wearable technologies,” *Global Challenges*, vol. 4, no. 7, p. 1 900 092, 2020.
- [12] Z. Li, K. Zheng, Q. Wang, *et al.*, *Screen-printing of carbons/conductive polymer composite inks for smart glove with high-performance textile sensors*. 2025. DOI: 10.1021/acsami.5c06035.
- [13] C. Luo, B. Tian, Q. Liu, Y. Feng, and W. Wu, *One-step-printed, highly sensitive, textile-based, tunable performance strain sensors for human motion detection*, 2020. DOI: 10.1002/admt.201900925.
- [14] J. D. Tocco, D. Presti, A. Rainer, E. Schena, and C. Massaroni, *Silicone-textile composite resistive strain sensors for human motion-related parameters*, 2022. DOI: 10.3390/s22103954.
- [15] Z. Yang, Y. Pang, X. Han, *et al.*, *Graphene textile strain sensor with negative resistance variation for human motion detection*. 2018. DOI: 10.1021/acsnano.8b03391.
- [16] M. Martínez-Estrada, I. Gil, and R. Fernández-García, *An alternative method to develop embroidery textile strain sensors*, 2021. DOI: 10.3390/textiles1030026.
- [17] A. Salam, D.-N. Phan, S. U. Khan, *et al.*, *Development of a multifunctional intelligent elbow brace (mieb) using a knitted textile strain sensor*, 2022. DOI: 10.5604/01.3001.0015.6457.
- [18] M. Janda, K. Rostás, S. Pretl, and J. Řeboun, *Method of connecting printed and embroidered conductive paths in smart textiles*, 2022. DOI: 10.1109/ISSE54558.2022.9812714.
- [19] S. Park, S. Ahn, J. Sun, *et al.*, *Highly bendable and rotational textile structure with prestrained conductive sewing pattern for human joint monitoring*, 2019. DOI: 10.1002/adfm.201808369.
- [20] X. Huang, L. Liu, Y. H. Lin, *et al.*, “High-stretchability and low-hysteresis strain sensors using origami-inspired 3d mesostructures,” *Science Advances*, vol. 9, no. 34, eadh9799, 2023.
- [21] M. Amjadi, A. Pichitpajongkit, S. Lee, S. Ryu, and I. Park, “Highly stretchable and sensitive strain sensor based on silver nanowire–elastomer nanocomposite,” *ACS nano*, vol. 8, no. 5, pp. 5154–5163, 2014.
- [22] J. T. Muth, D. M. Vogt, R. L. Truby, *et al.*, “Embedded 3d printing of strain sensors within highly stretchable elastomers,” *Advanced materials*, vol. 26, no. 36, pp. 6307–6312, 2014.
- [23] L. Cha, S. Groß, S. Mao, T. Braun, S. Haddadin, and L. He, “Stretchable capacitive and resistive strain sensors: Accessible manufacturing using direct ink writing,” in *2025 IEEE 8th International Conference on Soft Robotics (RoboSoft)*, IEEE, 2025, pp. 1–6.
- [24] S. Rosset and H. R. Shea, “Flexible and stretchable electrodes for dielectric elastomer actuators,” *Applied Physics A*, vol. 110, no. 2, pp. 281–307, 2013.
- [25] H.-R. Tränkler and L. M. Reindl, *Sensortechnik: Handbuch für Praxis und Wissenschaft*. Springer-Verlag, 2015.